Supporting Information

Measurement report: Hygroscopicity of Size-Selective Aerosol Particles at Heavily Polluted Urban Atmosphere of Delhi: Impacts of Chloride Aerosol

Anil Kumar Mandariya[1,2], Ajit Ahlawat[3], Mohd. M. V. Haneef[1], Nisar A. Baig[1], Kanan Patel[4], Joshua S. Apte[5], Lea Hildebrandt Ruiz[4], Alfred Wiedensohler[3]*, and Gazala Habib[1]*

[1]Department of Civil Engineering, Indian Institute of Technology Delhi, New Delhi, India

[2]now at: Univ Paris Est Creteil and University Paris Cité, CNRS, LISA, F – 94010 Créteil, France

[3]Leibniz Institute for Tropospheric Research (TROPOS), Permoserstraße, 15 Leipzig, Germany

[4]Department of Civil, Architectural and Environmental Engineering, The University of Texas at Austin, Austin, Texas, USA

[5]McKetta Department of Chemical Engineering, The University of Texas at Austin, Austin, Texas, USA

Correspondence to: Gazala Habib (gazalahabib@civil.iitd.ac.in) and Alfred Wiedensohler (ali@tropos.de)

Content:

Number of Pages: 9

Number of Figures: 11

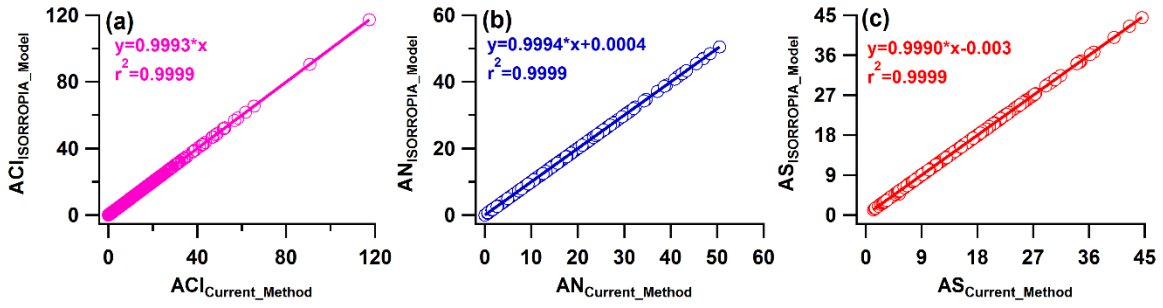

Figure S1: Regression plots between the calculated (a) ammonium chloride (ACl), (b) ammonium nitrate (AN), and (c) ammonium sulfate (AS) using ISORROPIA model and current modified ion-pairing scheme

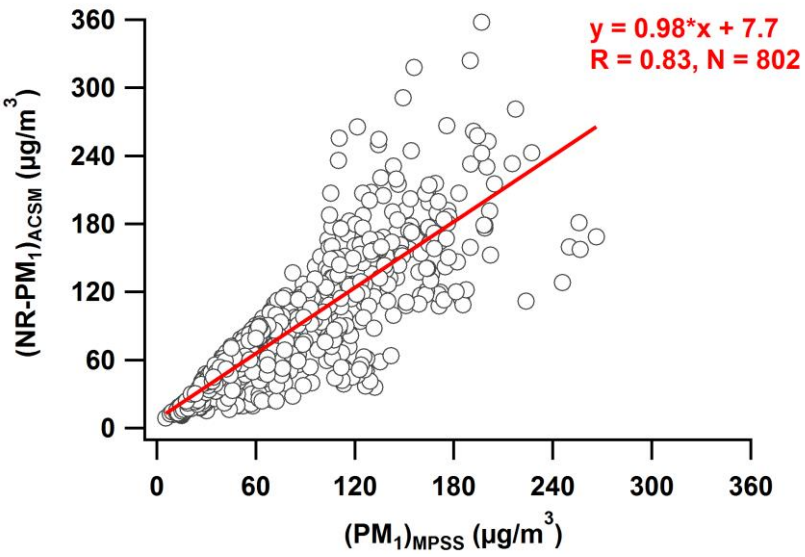

Figure S2: Mass closure between non-refractive PM_1 and PM_1 measured from ACSM and MPSS, respectively

S.1 Details on PMF Analysis:

S.1.1 Prior to the analysis,

1. spikes were removed from the dataset
2. the mass fragments with "bad" SNR (<0.2) were removed from the data set
3. the mass fragments with "weak" SNR (0.2-2) were down weighted
4. the contributions at m/z 44, 18, 17 and 16 were down weighted because of their linear correlation from the standard fragmentation table

S.1.2 Next,

- the number of factors were varied from one to five in the PMF tool
- the reduction in the ratio of the summation of scaled residuals (Q) to their expected value (Qexpected=$mn-p(m+n)$, where m corresponds to number of time steps (rows) and n corresponds to number of m/z (columns) in the input matrix, and p corresponds to the number of factors) "Q/Qexpected" was considered to determine the number of factors. The solution where the addition of further factors led to little reduction in it was explored
- increasing the number of factors beyond this point yielded unreasonable factor mass spectra due to factor splitting.
- Different different SEED values (from 0 to 10) were explored to understand the effect of different pseudo random starts

- Different FPEAK values (from -1 to 1) were explored to understand the rotational freedom of solutions respectively.

We found a four-factor solution (hydrocarbon-like OA, “HOA”; oxidized biomass burning OA, “BBOA”; less-oxidized OA, “LO-OOA”; more-oxidized OA “MO-OOA) to best represent the data set. HOA mass spectra (MS) correlated well with reference (Ulbrich et al., 2009; Ng et al., 2011) HOA spectra (pearson $R > 0.9$) and BBOA MS correlated well with reference BBOA spectra (pearson $R > 0.9$) (see Fig S1 for MS and Fig S2 for correlation with reference spectra). While both MO-OOA and LO-OOA correlated well with reference OOA and LVOOA factors, MO-OOA was highly oxidated ($f44 = 0.2$ compared to a value of 0.14 for LO-OOA). Further, SEED=0 and FPEAK = 0 were chosen because non-zero values either had no significant effect on the solution or led to unreasonable factor MS/factor splitting.

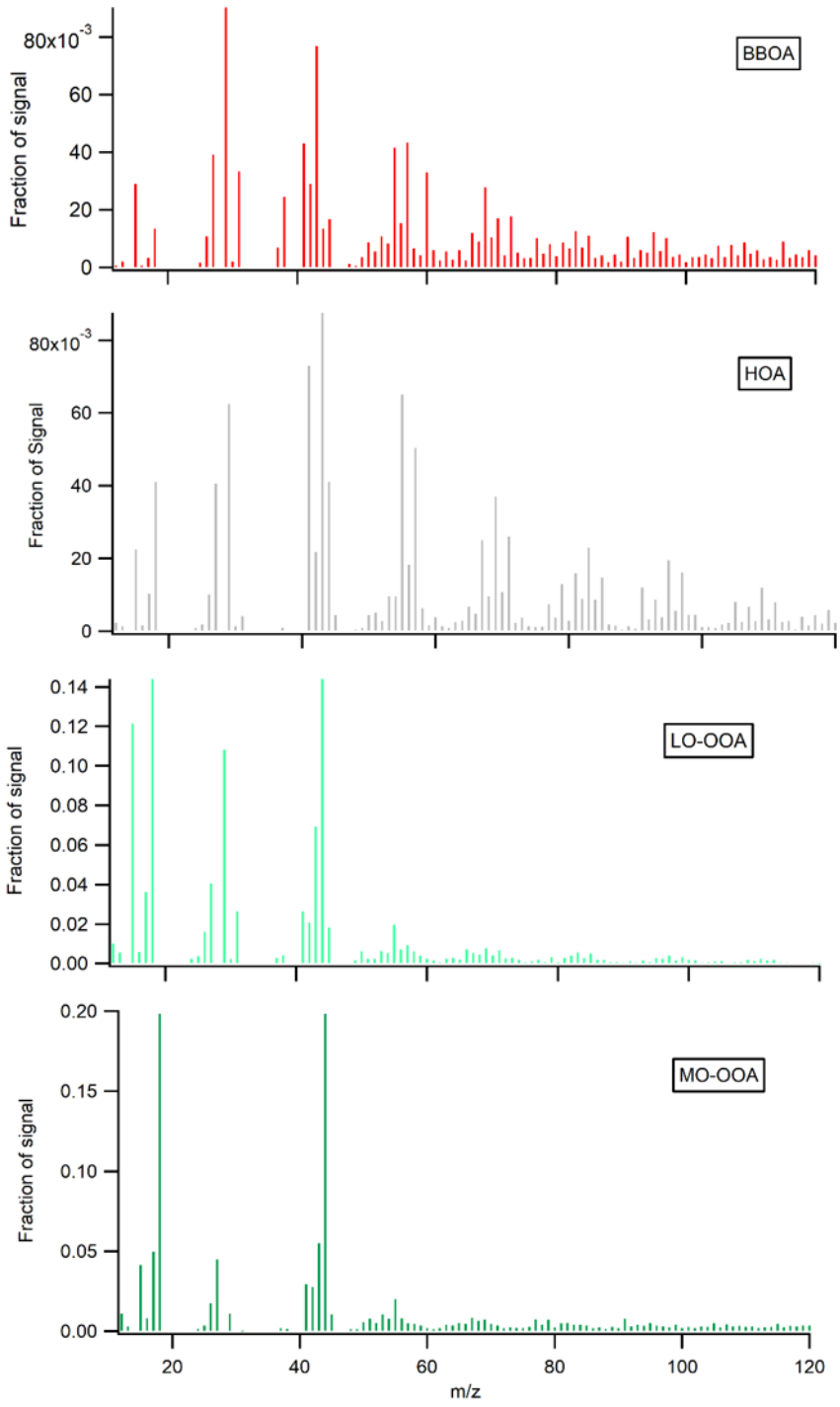

Figure S3: Mass spectra of the PMF factors

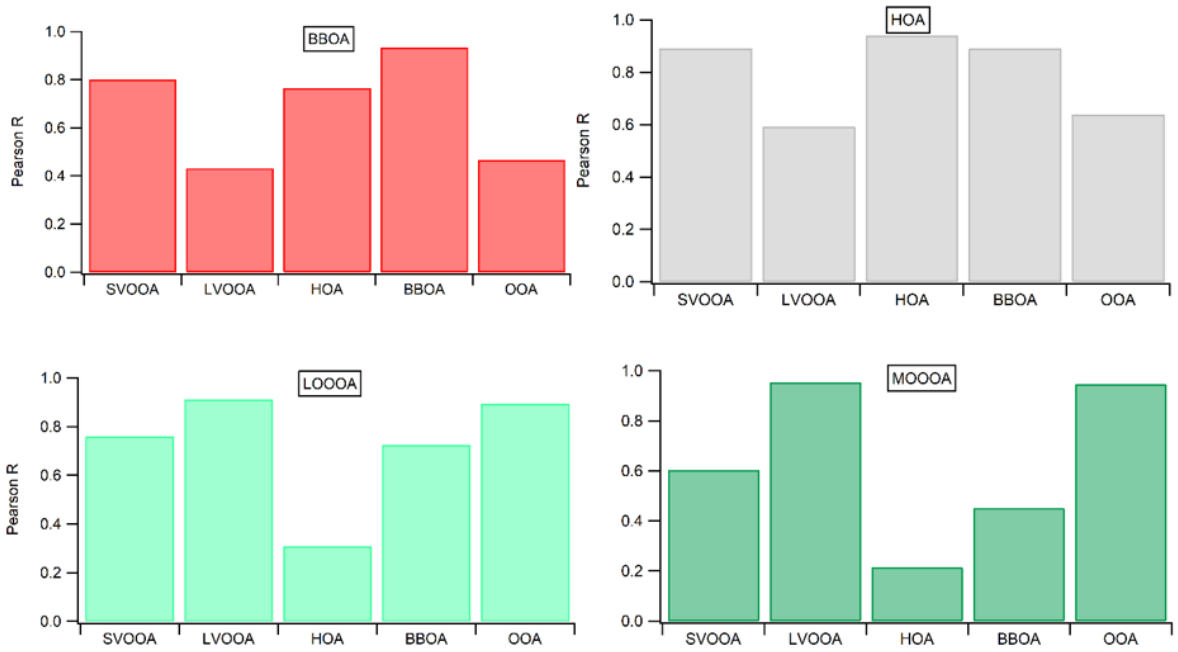

60

61 **Figure S4: Correlation of PMF factor mass spectra with reference mass spectra**

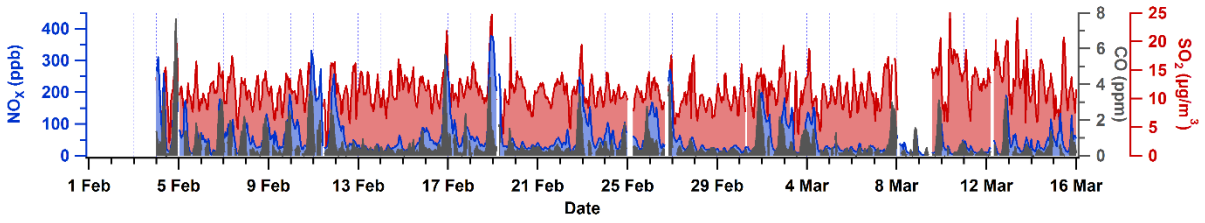

62

63 **Figure S5 Temporal variability in atmospheric NO_x, CO, and SO_2 gases concentrations.**

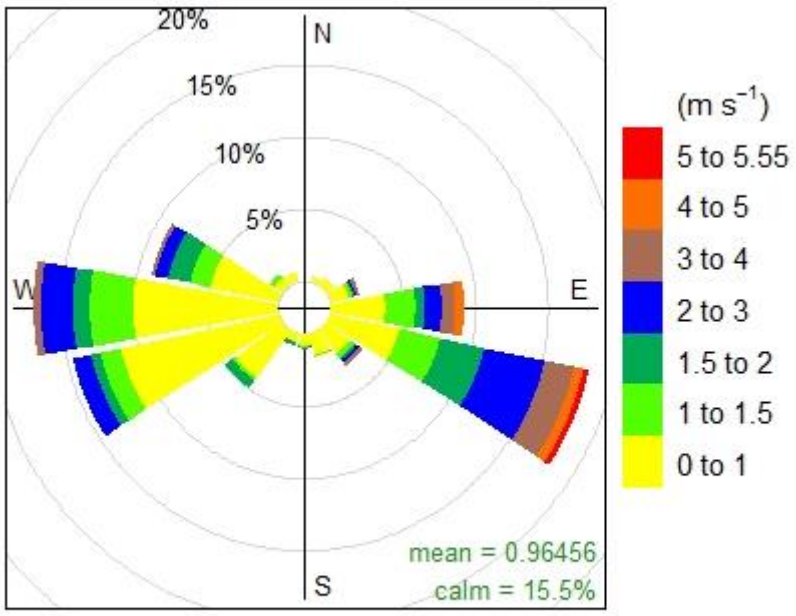

64

65 **Figure S6: Wind rose plot of hourly resolved wind speed (m/s) and wind direction (degree).**

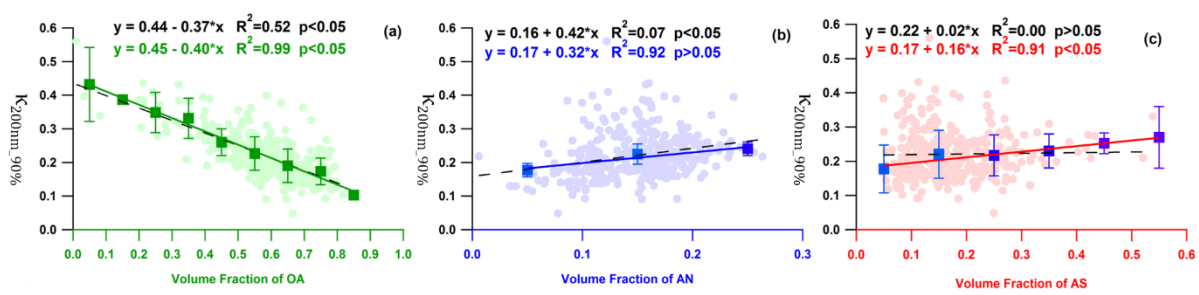

66

67 **Figure S7: Correlation plot for (a) $\kappa_{200nm\_90\%}$ vs volume fraction of organic aerosol (VF_{OA}), (b) $\kappa_{200nm\_90\%}$ vs volume**

68 **fraction of ammonium nitrate (VF_{AN}), and (c) $\kappa_{200nm\_90\%}$ vs volume fraction of ammonium sulfate (VF_{AS}).**

69

70

71

72

73

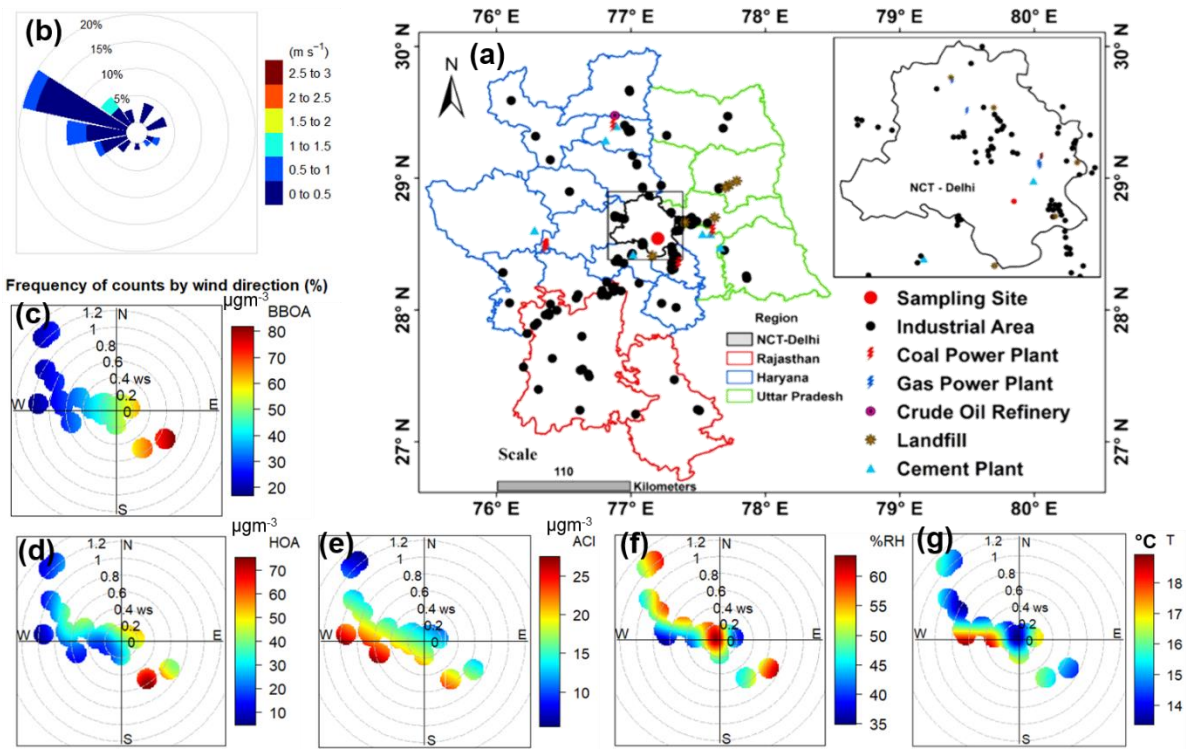

74

75 **Figure S8: Map of (a) Delhi showing various types of industries located in the region and nearby locations, (b) wind**
76 **rose diagram and conditional bi-polar plots showing variation in mass concentration of (c) biomass burning OA**
77 **(BBOA), (d) hydrocarbon like OA (HOA), (e) ammonium chloride (ACl), (f) % ambient relative humidity (RH), and**
78 **(g) ambient temperature (T), with wind direction (WD) and wind speed (WS) during H-BB events. A background map**
79 **showing various industrial locations was adapted from Rai et al. (2020).**

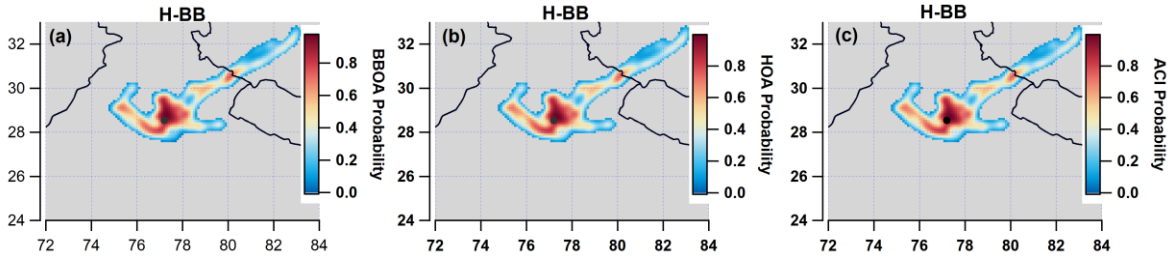

80

81 **Figure S9: Association of the mass concentration of various chemical species (a) biomass burning OA (BBOA), (b)**
82 **hydrocarbon like OA (HOA), (c) NH_4Cl (ACl) of PM_1 with 48 hr air mass back trajectories (BT) for H-BB period.**

83

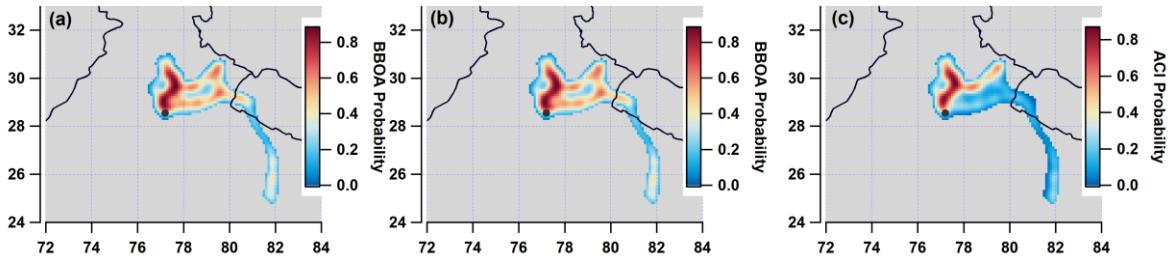

Figure S10: Association of the mass concentration of various chemical species (a) biomass burning OA (BBOA), (b) hydrocarbon like OA (HOA), (c) NH_4Cl (ACl) of PM_1 with 48 hr air mass back trajectories (BT) for H-HOA period.

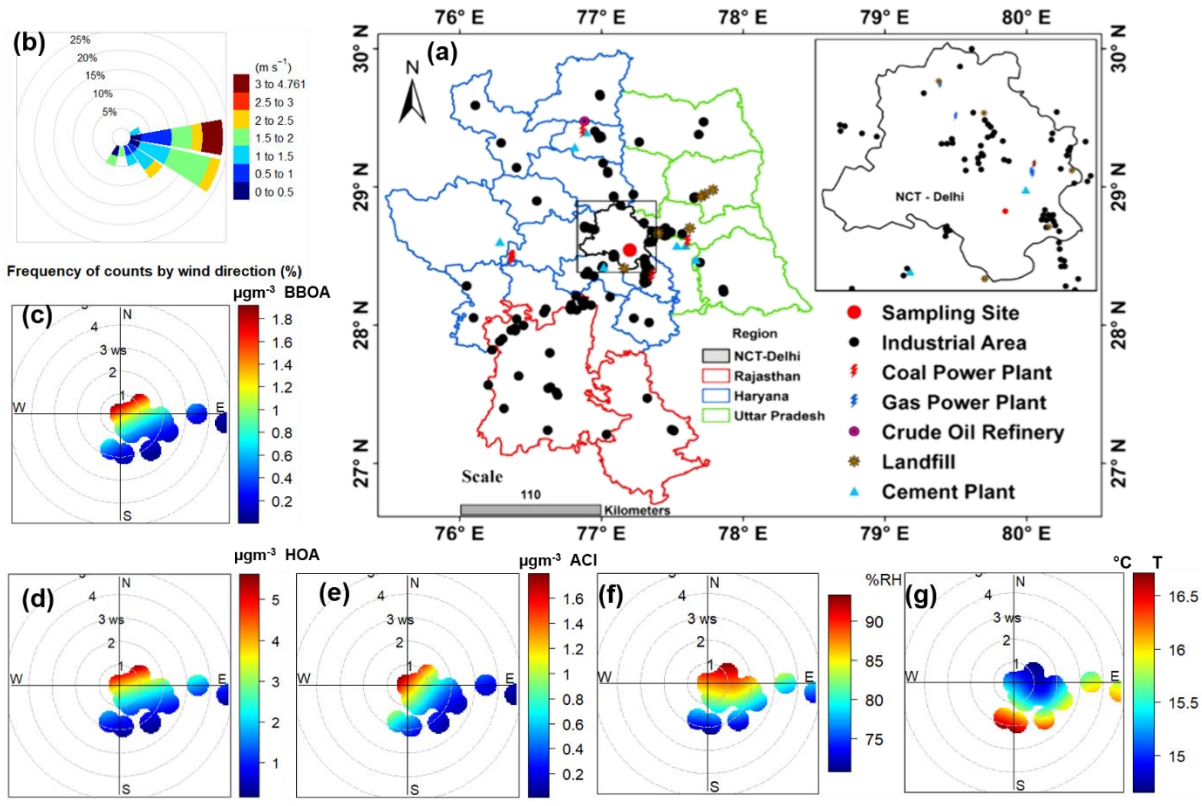

Figure S11 Map of (a) Delhi showing various types of industries located in the region and nearby locations, (b) wind rose diagram and conditional bi-polar plots showing variation in mass concentration of (c) biomass burning OA (BBOA), (d) hydrocarbon like OA (HOA), (e) ammonium chloride (ACl), (f) % ambient relative humidity (RH), and (g) ambient temperature (T), with wind direction (WD) and wind speed (WS) during relatively Clean periods. A background map showing various industrial locations was adapted from Rai et al. (2020).

95 References

96 Rai, P., Furger, M., El Haddad, I., Kumar, V., Wang, L., Singh, A., Dixit, K., Bhattu, D., Petit, J.-E., Ganguly,
97 D., Rastogi, N., Baltensperger, U., Tripathi, S. N., Slowik, J. G. and Prévôt, A. S. H.: Real-time measurement
98 and source apportionment of elements in Delhi's atmosphere, Sci. Total Environ., 742, 140332,
99 doi:10.1016/j.scitotenv.2020.140332, 2020.

100